Sol-derived Hydroxyapatite Ddip-coating of a Porous Ti_6Al_4V Powder Compact

Mustafa Altındiş[1], Mustafa Güden[2,3], Chaoying Ni[4]

[1]Materials Science and Engineering Program, Izmir Institute of Technology, Gulbahce Koyu, Urla, Izmir, Turkey
[2]Department of Mechanical Engineering, Izmir Institute of Technology, Gulbahce Koyu, Urla, Izmir, Turkey
[3]Center for Materials Research, Izmir Institute of Technology, Gulbahce Koyu, Urla, Izmir, Turkey
[4]Department of Materials Science and Engineering, Dupont Hall, University of Delaware, Newark, DE 19716, USA

Abstract

A sintered porous Ti_6Al_4V powder compact with a mean pore size of 63 μm and an average porosity of 37±1% was dip-coated at soaking times varying between 1- and 5-minute using a sol-derived calcium Hydroxyapatite (HA) powder. The coated compacts were heat-treated at 840 °C. The coating thickness was found to increase with increasing soaking time, from 1.87 μm at 1-minute soaking to 9 μm at 5-minute soaking on the average. It was shown that at increasing soaking times, the originally open pores started to close, while at low soaking times the Ti_6Al_4V particles were partially coated. The coating layer was shown to be nano porous and the depth of coating was observed to be relatively shallow: only few particles near the compact surface were HA-coated.

Introduction

The application of porous components of biocompatible Ti and Ti_6Al_4V alloy is to provide better interaction with bone due to the higher degree of bone in-growth and body fluid transport through three-dimensional interconnected array of pores[1], leading to improved implant fixation. Furthermore, the relatively low elastic moduli of porous metals as compared with those of bulk metals reduce the extent of stress shielding causing implant loosening [2]. The sintering powder compacts and the space holder methods were previously applied successfully to produce biocompatible open-cell Ti and Ti_6Al_4V powder compacts and foams, respectively [3-7]. Both methods, the sintering powder compacts and the space holder methods, allow the direct near net-shape fabrications of porous implant components having elastic modulus values comparable with that of natural bone, relatively homogeneous pore structures and high level of porosities (30-70%) [3, 5, 6]. The porosity level of sintered Ti compacts suitable for the bone replacement was found around 30%, which was in accord with the proposed optimal porosity for the ingrowths of new-bone tissues[5, 8, 9]. However, the compressive yield strength of sintered Ti compacts was shown to be lower than that of the human cortical bone due to the relatively low yield strength of Ti powder used [5]. The use biocompatible stronger Ti alloy powders such as Ti_6Al_4V, which is widely used in biomedical applications, increased the yield strength of powder compacts [3].

Ti is known to be a bioinert material and it cannot directly bond to living bone directly [10]. Calcium Phosphate (CaP) coating of porous surfaces including Ti mesh [11, 12] and the sintered powder (beads) surface coatings [13, 14] has beneficial effects on the bone-generating properties, improving the implant fixation to bone. The aim of this study is to investigate the effect of dip-coating soaking time on the hydroxyapatite (HA) coating layer thickness of a Ti_6Al_4V sintered powder compact. The selected sol-derived powder dip-coating method is relatively simple, inexpensive and suitable for the mass production. Ti_6Al_4V powder compacts were prepared in house using a powder metallurgical-sintering route and originally developed for the hard tissue replacement applications such as spinal cages used in spinal surgery.

Materials and Method

The sintered powder compacts were prepared using atomized spherical Ti_6Al_4V alloy powders

*corresponding author. E-mail: mustafaguden@iyte.edu.tr

 Printed in Kazakhstan

(Phelly Materials Company), complied with ASTM 1580-1 standard [15]. The powder particle size ranged between 100 and 200 μm with a mean particle size of 157 μm. The green powder compacts were compacted uniaxially at room temperature at 400 MPa, using a polyvinyl alcohol solution (5-10% by volume) as binder. The sintering of the compacts was conducted at 1200°C for 2h under high purity Ar atmosphere. The details of the compact preparation are given in elsewhere [3]. The compact contained 100% three-dimensional interconnected pores with pore sizes ranging between 16 and 200 μm, a mean pore size of 63 μm and an average porosity of 37±1%. The sintering of the needle-like α-phase (acicular alpha) of the starting powder resulted in the formation of so-called Widmanstätten microstructure (α+β). The elastic modulus and compressive yield strength varied between 4 and 6 GPa and 155 and 175 MPa, respectively [3], satisfying the strength and modulus requirements for certain hard-tissue replacements such as spinal cages used for bone ingrowth in patients with spinal trauma, tumors and degenerative diseases.

The HA powder for the dip coating solution was prepared according to the protocol developed by Maviş and Taş[16], which was essentially a modified route of chemically precipitated calcium HA powder processing originally proposed by Hayek and Newesely in 1963[17]. A 3 ml aliquot of 0.1 g/l methyl cellulose solution (99% pure, Sigma, St. Louis, MO) acting as dispersant was mixed with 1440 ml of deionized water. Thereafter, 0.152 mol of $Ca(NO_3)_2{\cdot}4H_2O$ (99% pure, Merck, Darmstadt, Germany) and 0.091 mol of $(NH_4)_2HPO_4$ (99% pure, Merck) were dissolved with above solution sequentially (Ca/P=1.67). This mixing step resulted in formation of an opaque solution mixture. Finally, 115 ml of 28-30 vol% NH_4OH (99% pure, Performans, Turkey) was added to the final opaque solution and pH of the solution was kept around 10. Then, the solution was heated to the temperature range of 60-70°C on a hot plate for 90 min. The precipitates formed were vacuum filtered using Buchner funnel, washed with distilled water for several times and then dried in an oven at 90°C for 6 h. Above procedure of HA powder processing was found to yield a single phase HA at relatively high temperatures, up to 1200-1300 °C [16, 18].

The used dip-coating solution composition in wt% was as follows: 7.3% HA powder, 66.2% ethanol (99.9% pure), 13.8% distilled water, 10.2% glycerol (98.5% pure, Performans), 2.2% Poly(ethylene glycol) (99.5% pure, molecular weight of 15 000, Merck), 0.3% gelatin (99.9% pure, Merck, Darmstadt, Germany). The dip-coating solution composition was previously shown to form a crack free thick HA coating on Ti_6Al_4V strips with a dipping and removal rate of 100 mm/min [16].

Dip-coating of the cylindrical compacts, ~15 mm in diameter and ~10 mm in height, were performed in a dip coater at soaking times from 1 to 5-minute with one minute interval (dipping and removal rate of 100 mm/min). The compacts were heat-treated after dip-coating under Ar atmosphere (to prevent the oxidation of the Ti64 particles) at a temperature of 840 °C (2 h of peak soaking time), with a heating and cooling rate of 2 °C/min. The microscopic analysis on the coated compact samples was performed using a Nikon Eclipse L150 optical microscope and a Philips XL30-SFEG scanning electron microscope (SEM) with an Energy Dispersive X-ray (EDX). The polished cross-sections of epoxy-mounted coated compact samples were etched with Kroll's reagent (3 cm^3 of HF and 6 cm^3 of HNO_3 in 100 ml of H_2O) and used for the determination of the thickness and depth of the coating. A Philips X'pert X-ray diffraction (XRD) instrument with Cu-Kα radiation was used for the phase determination.

Results

The synthesized HA precursor powder used for dip-coating solution yielded stable dip- coating solution against the sedimentation as previously noted [16]. Initially, the powder was heat treated at various temperatures until 1200 °C for 2 h in order to determine the effect of temperature on the crystallinity of the powder. XRD spectra of the sol-derived HA powder as function of heat treatment temperature is shown in Figure 1. The phase composition of sol-derived powder was identified as low crystalline HA at 90 °C. The heat-treatment at higher temperatures however improves the crystallinty of the powder and the powder remains single-phase until about relatively high temperatures, 1200 °C, as noted previously in refs. [16, 18]. The powder XRD data shown in Figure 1 are agreed closely with the hexagonal structure of calcium HA (JCPDS-4-932). The hexagonal unit cell parameters of the powder heat-treated at 840 °C are calculated as; a=0.949 nm and c= 0.695 nm. The HA powder coated compacts was however heat treated at a temperature of 840 °C, below the α+β phase transition temperature [19]. The transmission electron micrograph of the synthesized

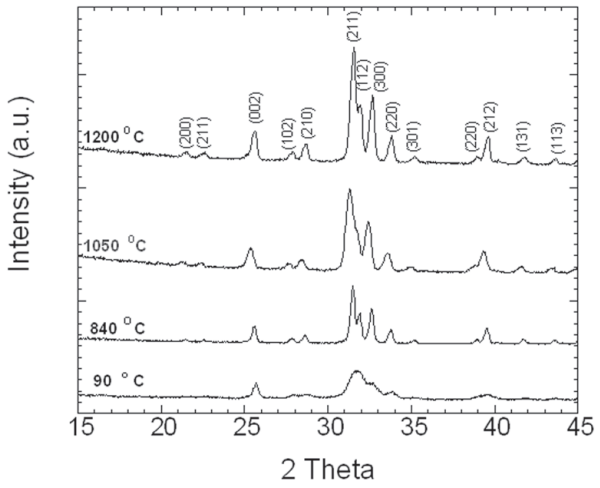

Fig. 1. XRD spectra of the sol-derived HA powder as function of heat treatment temperature.

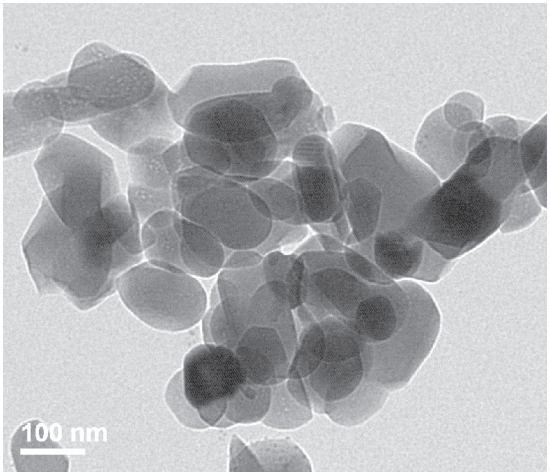

Fig. 2. Transmission electron microscopy micrograph of sol-derived HA powder.

sol-derived HA powder heat-treated at 840 °C is shown in Figure 2. The particles in Figure 2 are mostly elliptical in shape with the sizes of 100-200 nm.

The schematic of a coated powder compact sample is shown in Figure 3(a). In the SEM analysis of the coating layer, the pictures were taken from the cylindrical compact sample surface from the region A of Figure 3(a). The surface SEM picture of the powder compacts coated with sol-derived powder at 1-minute soaking time is further shown in Figure 3(b). The coating at particles sintering necks is relatively thick as marked with white arrows in Figure 3 (b). It is also noted in the same micrograph that particles are not completely coated with HA and cracks in the coating at sintering necks are clearly seen. Relatively large pores are still open, while small pores are closed after coating. The surface SEM micrographs of the coated samples at 2, 3, 4 and 5-minute soaking times are sequentially shown in Figures 3(c)-(f) for comparison. As seen in Figures 3(b-f), the surfaces of Ti_6Al_4V particles are almost completely coated until about 3-minute soaking, except small regions on the top of the particles as marked with arrows in Figures 3(c) and (d). At 4-minute soaking, the HA coating starts to fill the originally open pores between sintered particles (Figure 3(e)). The pores are almost completely closed when the soaking time increases to 5-minute (Figure 3(f)). Large cracks are also seen on the coating layer particularly near the sintering necks as marked by arrow in Figure 3(f). In all dip-coated compact samples, the coating started from the sintering necks of the particles and proceeded to the uncoated regions. Therefore; as stated earlier, the coating layer is thicker at the particle sintering necks as marked with white arrows in Figure 4, a similar observation was previously noted in a Ti-bead coated Ti implant[20]. Accompanying extensive microscopic observations on the sintering necks revealed that the coating thickness differences between the sintering necks and the particle surface and the extent of coating cracks at the sintering necks decreased as the soaking time increased from 1 to 3-minute.

The crystal size of the heat-treated powder was microscopically determined from the coated and heat-treated compact samples. The SEM micrograph of a coated (3-minute soaking) and heat-treated compact sample surface is shown in Figure 5(a). The coating layer in Figure 5(a) clearly proves the formation of a nanoporous coating layer on Ti_6Al_4V particles following the heat treatment process at 840 °C. The pore size of the coating layer is comparable with HA particle size, in 100 nm's sizes. The EDX analysis on the coating layer after heat treatment at 840 °C gives a Ca and P ratio of 1.67 as depicted in Figure 5(b).

The variation of the thicknesses of the coating layer as function soaking time was determined microscopically from Ti_6Al_4V particles adjacent to the coating layer. For that, the coated compact samples were epoxy impregnated and then cut perpendicular to the cylinder flat surface (A in Figure 3(a)) through mid-section. Figures 6(a-e) show sequentially the coating layers on the particles after 1,2,3,4 and 5-min soaking times. The particle, coating layer and

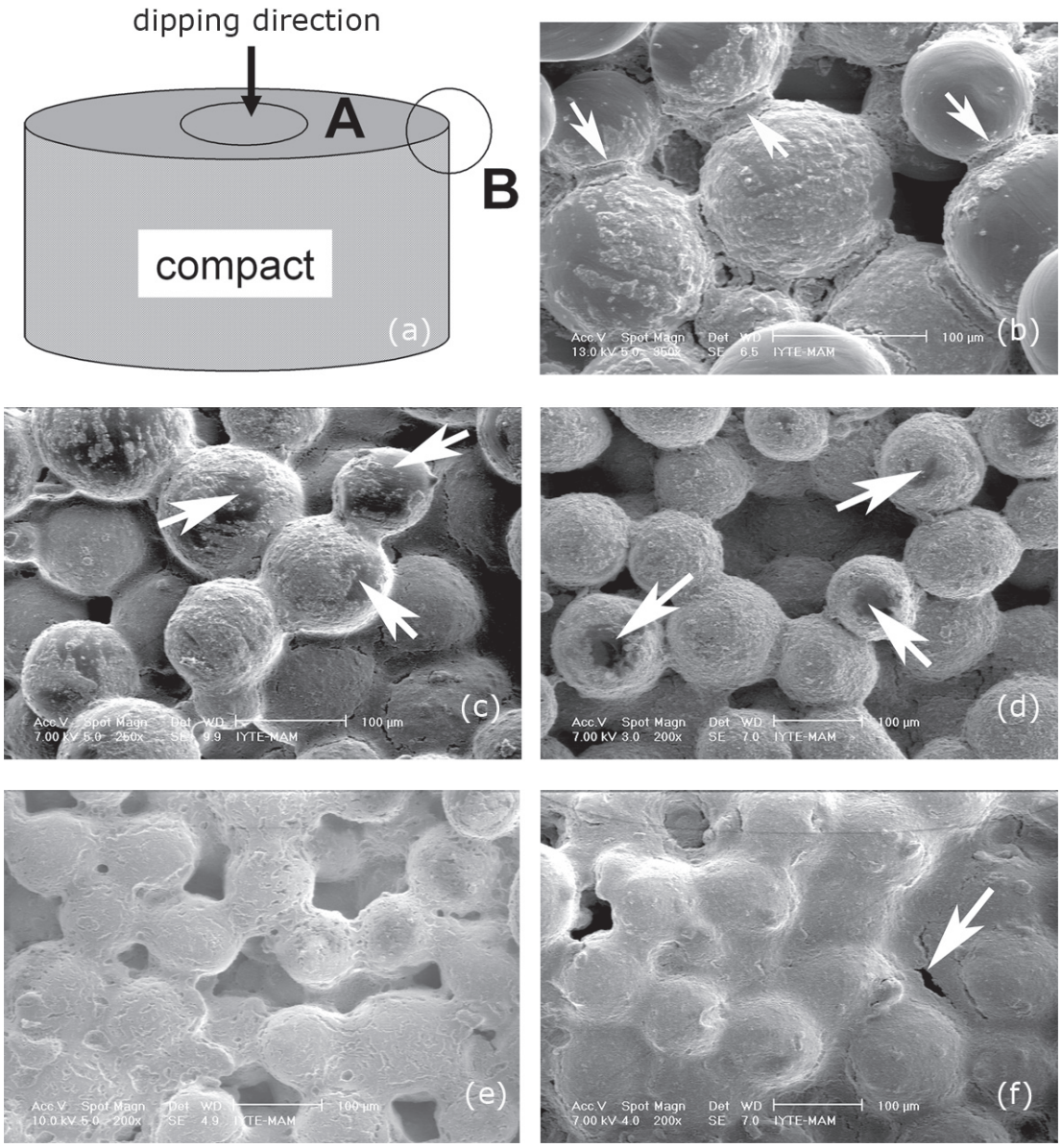

Fig. 3. Schematic of a coated compact sample (a) and the surface SEM micrographs of sol-derived HA powder coated compact samples after (b) 1-, (c) 2-, (d) 3-, (e) 4- and (f) 5-minute soaking time and heat-treatment at 840 °C.

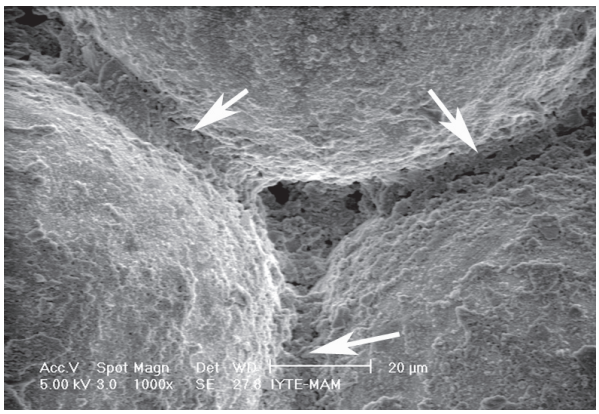

Fig. 4. SEM micrograph showing thicker HA coating at the particle sintering necks after 3-minute soaking time and heat-treatment at 840 °C.

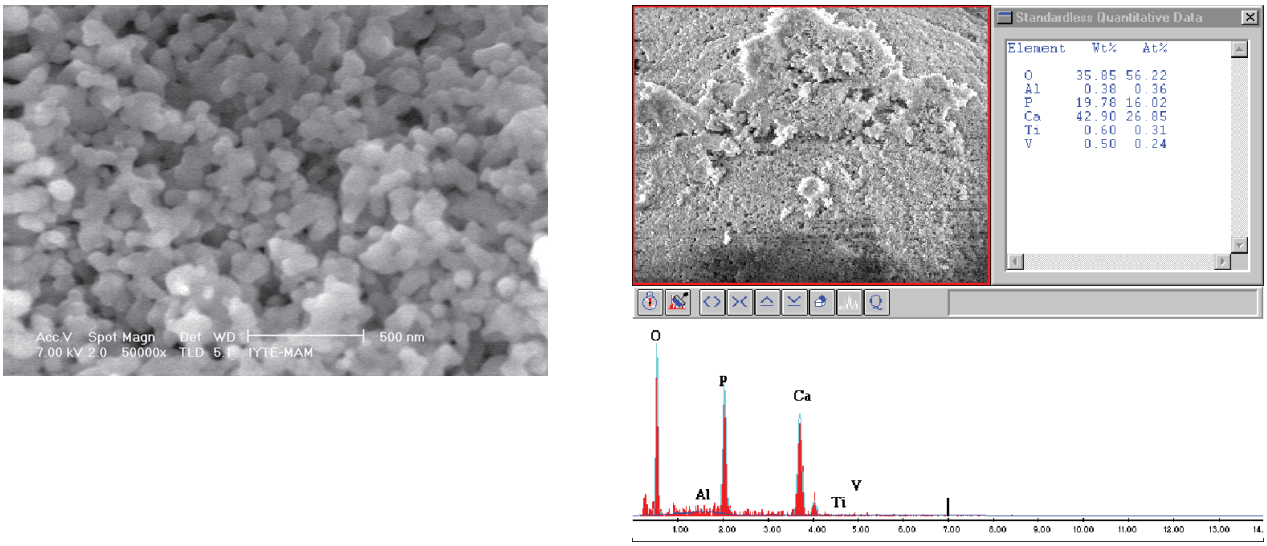

Fig. 5. (a) SEM micrograph showing nano porous HA coating layer on a Ti_6Al_4V particle in a coated compact sample and (b) EDX analysis of HA coating layer (3-minute soaking time and heat-treatment at 840 °C).

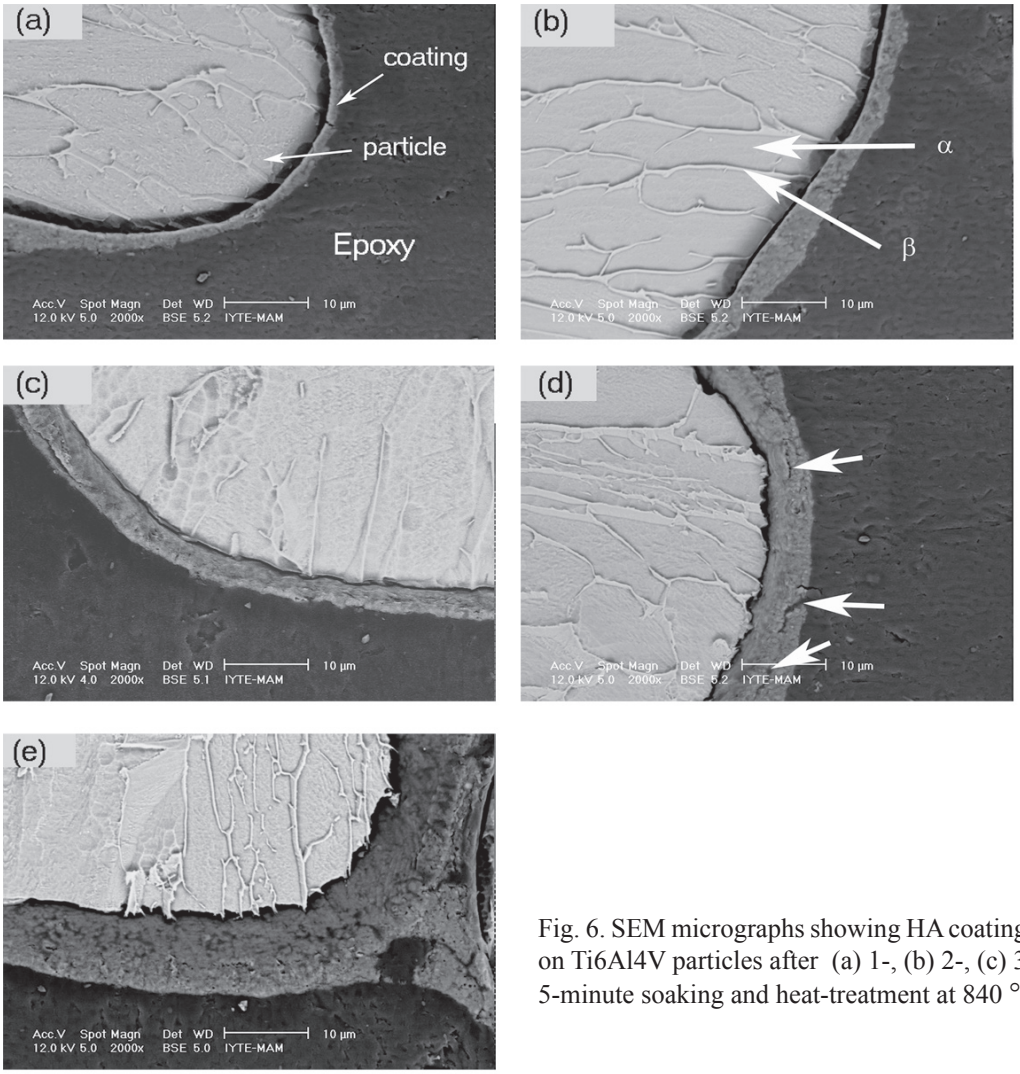

Fig. 6. SEM micrographs showing HA coating layer thickness on Ti6Al4V particles after (a) 1-, (b) 2-, (c) 3-, (d) 4- and (e) 5-minute soaking and heat-treatment at 840 °C.

epoxy layer are marked with arrows in Figure 6(a). As the soaking time increases the coating layer thickness increases as seen in Figures 6(a-e). The cracks in the coating layer are clearly seen in the micrograph of Figure 6(d) (marked with arrows). It is also noted that the coating layer is delaminated from the particle surface, partly arising from the attack of the chemical etching reagent used. In Figure 6(b), the Widmanstätten microstructure of the sintered Ti_6Al_4V particles, composing β lathes (bcc and rich in V) and α platelets (hcp and rich in Al) is also seen.

In spite of the thicker coating layer formation near sintering necks, the coating layer thickness on the particles is considered to be relatively homogenous. The variation of HA coating layer thickness as function of soaking time is shown in Figure 7. At least 8 measurements were taken for each soaking time. The coating thickness shown in Figure 7 increases with increasing soaking time, from 1.87 μm at 1-minute soaking to 2.95 μm at 2-minute, 4.15 μm at 3-minute, 5.66 μm at 4-minute and 9 μm at 5-minute soaking time on the average.

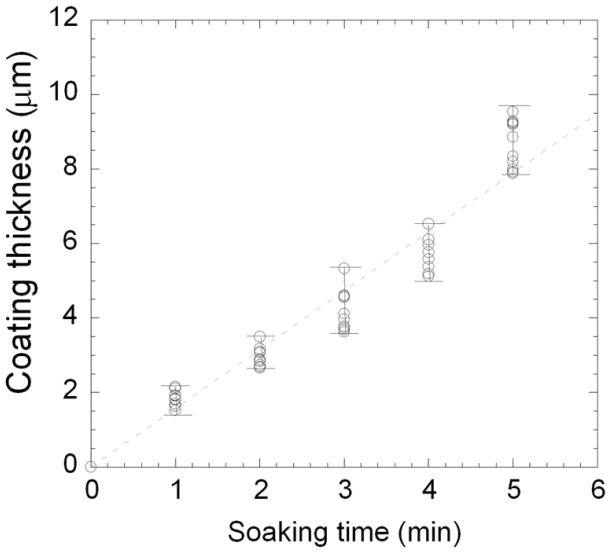

Fig. 7. The thickness of HA coating as a function of soaking time.

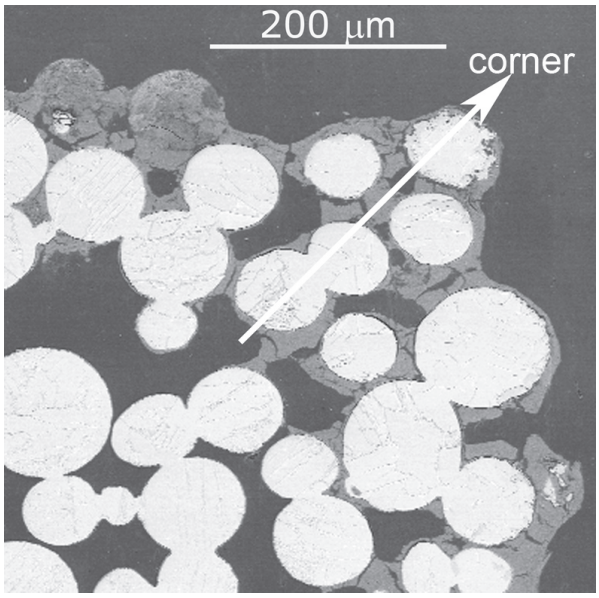

Fig. 8. SEM micrograph of the cross-section of HA coated compact sample after 5-minute soaking and heat-treatment at 840 °C.

Discussion

The synthesized sol-derived HA powder used in this study was found to be partially crystalline after drying at 90°C and were single-phase and crystalline until about 1200°C. Thermal treatment temperature following the coating should however be selected at a minimum level that still assures sufficient quality of HA film, in terms of crystallinity, film integrity, and adhesion to the substrate. Furthermore, the lower sintering temperatures also avoid α+β phase transition occurring at 883 and 960 °C in titanium and titanium alloy, respectively[19]. This ensures the retention of the starting material microstructure; and hence allowing to controlling the microstructure development. Based on the above facts, the sintering of compacts coated with sol-derived and commercial HA powders were performed at 840 °C, below α+β phase transition temperature.

The thicker deposit at the sintering necks is attributed to be due to capillary effects drawing the coating solution into this concave region. The sinter necks have a concave geometry with the radius of curvature of the concavity being small (Figure 4). Cracks on the coating layer are likely resulting from the greater residual stresses that develop within these thicker film regions. Future studies are therefore required to optimize the soaking-time as function of crack formation on the coating layer. It was previously shown that the bone in-growth occurred between

the delaminated calcium phosphate layer and the substrate in a Ti implant coated with Ti beads; furthermore, the extent of bone in-growth or fill within the sintering necks increased in the presence of the calcium phosphate film[13]. Therefore, the cracks and delaminations formed at the sintering necks are believed to not significantly impair the bone in-growth behavior of the studied compacts. Furthermore, epoxy-mounted coated compacts were sectioned longitudinally in order to determine the depth of the coating and the openness of the pores. In Figure 8, the cross-section of a coated sample at 5-minute soaking time is shown near the corner of the sample (B in Figure 3(a)). The coating depth from the compact surface is seen in this figure relatively small (300 μm), proving that only two-three particles near the compact surface are coated. The same shallow depth of coating was also observed in compacts coated at different soaking times, proving that few Ti_6Al_4V particles near the compact surface were HA-coated.

The present results have shown that the dip-coating soaking time has a great effect on the film thicknesses and the openness of pores particularly at the surface. The soaking times until about 3-minute are sufficient to form a relatively thick HA layer on Ti_6Al_4V particles. Nevertheless, the effects of certain microstructural features including coating layer thickness, coating depth and the coating defects on bone in-growth properties of the powder compacts should be further assessed.

Conclusions

In this study, the effect of dip-coating soaking time on the HA coating layer thickness of a Ti_6Al_4V sintered powder compact was investigated. The sintered powder Ti_6Al_4V compacts were prepared using a powder metallurgical-sintering route with a mean pore size of 63 μm and an average porosity of 37±1%. The porous Ti_6Al_4V powder compacts were successfully dip-coated using sol-derived nano size HA powder until about the soaking times of 3-minute by considering uniformity of the coating layer and openness of the initial pores. The coating started from the particle sintering necks and cracks on the coating layer particularly at the sintering necks were observed in all dip-coated compact samples. Increasing soaking times however resulted in closing the originally open pores, while at lower soaking times the particles were partially coated. Finally, the coating layer was shown to be nano- porous, comprising nano size HA particles and pores.

Acknowledgements

This work has been supported by Hipokrat Medical Devices Manufacturing and Marketing Inc. of Turkey.

References

1. Pilliar, R.M., Journal of Biomedical Materials Research-Applied Biomaterials 21:1(1987).
2. Long, M. and H.J. Rack, Biomaterials 19:1621(1998).
3. Guden, M., E. Celik, E. Akar, and S. Cetiner, Materials Characterization 54:399(2005).
4. Guden, M., E. Celik, S. Cetiner, and A. Aydin, Advances in Experimental Medicine and Biology 553:257(2004).
5. Oh, I.H., N. Nomura, N. Masahashi, and S. Hanada, Scripta Materialia 49:1197 (2003).
6. Wen, C.E., M. Mabuchi, Y. Yamada, K. Shimojima, Y. Chino, and T. Asahina, Scripta Materialia 45:1147(2001).
7. Wen, C.E., Y. Yamada, K. Shimojima, Y. Chino, T. Asahina, and M. Mabuchi, Journal of Materials Science-Materials in Medicine 13:397(2002).
8. Oh, I.H., N. Nomura, and S. Hanada, Materials Transactions 43:443-446(2002).
9. Oh, I.H., H. Segawa, N. Nomura, and S. Hanada, Materials Transactions 44:657(2003).
10. Hench, L.L., Journal of the American Ceramic Society 74:1487(1991).
11. Tsukeoka, T., M. Suzuki, C. Ohtsuki, Y. Tsuneizumi, J. Miyagi, A. Sugino, T. Inoue, R. Michihiro, and H. Moriya, Journal of Biomedical Materials Research Part B-Applied Biomaterials 75B:168(2005).
12. Vehof, J.W.M., P.H.M. Spauwen, and J.A. Jansen, Biomaterials 21:2003(2000).
13. Nguyen, H.Q., D.A. Deporter, R.M. Pilliar, N. Valiquette, and R. Yakubovich, Biomaterials 25:865(2004).
14. Tache, A., L. Gan, D. Deporter, and R.M. Pillar, International Journal of Oral & Maxillofacial Implants 19:19(2004).
15. ASTM F 1580-95, Standard specification for titanium and Ti_6Al_4V alloy powders for coating surgical implants.

16. Mavis, B. and A.C. Tas, Journal of the American Ceramic Society 83:989(2000).
17. Hayek, E. and H. Newwsely, Inorganic Syntheses 7:63(1963).
18. Tas, A.C., F. Korkusuz, M. Timucin, and N. Akkas, Journal of Materials Science-Materials in Medicine 8:91(1997).
19. Rhodes, C.G., in Voort Vander (ed) Microscopy and titanium alloy development, New York: Van Nostrand Reinhold Company, 1986, p. 237.
20. Gan, L., H. Wang, A. Tache, N. Valiquette, D. Deporter, and R. Pilliar, Biomaterials 25:5313(2004).

Received 16 november 2009.